Article ID 1004-924X(2003)02-0114-06

Prediction of electromigration failure in passivated polycrystalline line

Kazuhiko Sasagawa[1], Masataka Hasegawa[2], Masumi Saka[2], Hiroyuki Abé[3]

(1. *Department of Intelligent Machines and System Engineering, Hirosaki University, 3 Bunkyo_cho, Hirosaki 036-8561, Japan; Tel& FAX: + 81_172_39_3675 E_mail: sasagawa@cc. hirosaki_u. ac. jp*
2. *Department of Mechanical Engineering, Tohoku University, 01 Aoba, Aramaki, Aoba_ku, Sendai 980_8579, Japan;*
3. *Tohoku University, 2_1_1 Katahira, Aoba_ku, Sendai 980_8577, Japan)*

Abstract: Recently, a governing parameter for electromigration damage in passivated polycrystalline lines, AFD^{*}_{gen}, was formulated considering the effect of the atomic density gradient. In this study, a prediction method for electromigration failure in a passivated polycrystalline line was proposed using AFD^{*}_{gen}. The characteristics of film used for prediction is established in advance using a method based on AFD^{*}_{gen}. The film characteristics of metal lines with different lengths were determined experimentally by AFD^{*}_{gen}_based method. From the film characteristics obtained, both lifetime and location of failure in the passivated polycrystalline lines were predicted through numerical simulation of failure process. Good agreement has been shown between the predicted and the experimental results concerning both lifetime and location of failure.

Key words: electromigration; passivated polycrystalline

CLC number: TN451 **Document:** A

1 Introduction

The latest progress in packaged silicon integrated circuits (ICs) is noteworthy. With the advance, however, some problems about the deterioration of the reliability have been raised. For instance, the higher current density due to scaling down causes electromigration in interconnect metal line. Electromigration is the transportation of the metallic atoms by electron wind. Voids are formed as a result of depletion of atoms, and hillocks are formed as a result of accumulation of atoms in the metal line. The growth of voids ultimately leads to metal line failure. To predict the electromigration failure is of significance from the viewpoint of ensuring the reliability of interconnect metal lines.

We have proposed an approach which makes use of a so_called governing parameter for electromigration damage. A parameter governing electromigration damage in uncovered polycrystalline and bamboo lines, AFD^{*}_{gen}, has been identified[1,2] and a method for failure prediction in these lines has been developed using AFD_{gen}[3,4]. In these studies, uncovered lines have been treated in order to build up a foundation for the development of a practical prediction method of electromigration failure. However, the metal lines used in IC are covered with passivation. In the covered metal lines, a stress distribution, or an atomic density distribution is built up and plays an important role in the mechanism of electromigration damage. Recently, a governing parameter, AFD^{*}_{gen}, for electromigration damage in a passivated polycrystalline line was

Received date: 2003-01-15; **Revised date:** 2003-03-05.

formulated by adding the effect of atomic density gradient to AFD^*_{gen}[5].

In this study, a prediction method for electromigration failure in a passivated polycrystalline line is proposed using AFD^*_{gen}. In advance of the prediction, a method to determine film characteristics used in the prediction is shown based on AFD^*_{gen}. The AFD^*_{gen}-based method is applied to the passivated metal line with different line lengths and the film characteristics of these lines are obtained experimentally. Based on the obtained film characteristics, both the lifetime and the failure location in the passivated polycrystalline lines are predicted by means of numerical simulation of the failure process, covering the building up of atomic density distribution, void initiation, void growth and ultimately line failure. The usefulness of this method is shown by comparison of predicted results with experimental ones.

2 Governing parameter for electromigration damage

The parameter governing electromigration damage, AFD^*_{gen}, has been proposed for a passivated polycrystalline line. The parameter AFD^*_{gen} was formulated as follows[3]:

$$AFD^*_{gen} = \frac{1}{4\pi}\int_0^{2\pi} (AFD_{gb}\theta) + |AFD^*_{gb}\theta|)\,d\theta, \tag{1}$$

where

$$AFD^*_{gb}\theta = C^*_{gb} N \frac{4}{\sqrt{3}d^2}\frac{1}{T} \exp\left\{-\frac{Q_{gb} + k\Omega(N - N_T)/N_0 - \sigma_T\Omega}{kT}\right\} \times \sqrt{3}\Delta\varphi\left\{(j_x\cos\theta + j_y\sin\theta) Z^*e\rho - \frac{K\Omega}{N_0}\left(\frac{\partial N}{\partial x}\cos\theta + \frac{\partial N}{\partial y}\sin\theta\right)\right\} - \frac{d}{2}\Delta\varphi \left\{\left(\frac{\partial j_x}{\partial x} - \frac{\partial j_y}{\partial x}\right) Z^* e\rho\cos 2\theta - \frac{k\Omega}{N_0}\left(\frac{\partial^2 N}{\partial x^2} - \frac{\partial^2 N}{\partial y^2}\right) \cos 2\theta + \left(\frac{\partial j_x}{\partial y} + \frac{\partial j_y}{\partial x}\right) Z^*e\rho\sin 2\theta - 2\frac{k\Omega}{N_0}\frac{\partial^2 N}{\partial x\partial y}\sin 2\theta\right\} - \frac{\sqrt{3}}{4}d\frac{k\Omega}{N_0}\left(\frac{\partial^2 N}{\partial x^2} + \frac{\partial^2 N}{\partial y^2}\right) - \frac{k\Omega/N_0}{kT} \left[\frac{\sqrt{3}}{4}d\left\{Z^*e\rho\left(j_x\frac{\partial N}{\partial x} + j_y\frac{\partial N}{\partial y}\right) - \frac{k\Omega}{N_0}\left(\frac{\partial N}{\partial x}\frac{\partial N}{\partial x} + \frac{\partial N}{\partial y}\frac{\partial N}{\partial y}\right)\right\} - \frac{d}{2}\Delta\varphi \left\{Z^*e\rho\left(j_y\frac{\partial N}{\partial x} + j_x\frac{\partial N}{\partial y}\right) - 2\frac{k\Omega}{N_0}\frac{\partial N}{\partial x}\frac{\partial N}{\partial y}\right\}\sin 2\theta\right] + \frac{\sqrt{3}d}{4T}\left\{\frac{Q_{gb} + k\Omega(N - N_T)/N_0 - \sigma_T\Omega}{kT} - 1\right\} \left\{Z^*e\rho\left(j_x\frac{\partial T}{\partial x} + j_y\frac{\partial T}{\partial y}\right) - \frac{k\Omega}{N_0}\left(\frac{\partial N}{\partial x}\frac{\partial T}{\partial x} + \frac{\partial N}{\partial y}\frac{\partial T}{\partial y}\right)\right\}, \tag{2}$$

and the constant C^*_{gb} denotes the product $D_0\delta/k$. Symbol D_0 is a prefactor, δ the effective width of the grain boundary, k Boltzmann's constant, N atomic density, d the average grain size, T the absolute temperature, Q_{gb} the activation energy for grain boundary diffusion, κ the effective bulk modulus, Ω the atomic volume, N_T the atomic density under tensile thermal stress σ_T, N_0 the atomic density under stress-free condition, $\Delta\varphi$ a constant related to the relative angle between grain boundaries, Z^* the effective valence, e the electronic charge and ρ temperature-dependent resistivity. The quantities j_x and j_y are components of the current density vector in Cartesian coordinates, x and y.

4 Determination of film characteristics

4.1 Method

The film characteristics included in the formulae of AFD^*_{gen} are d, $\Delta\varphi$, Q_{gb}, Z^*, C^*_{gb} and κ. The average grain size d, can be measured using focused ion beam (FIB) equipment. As far as φ is concerned, we use a value obtained from an uncovered metal line made of the same Al film as the covered metal line[3]. An AFD^*_{gen}-based method for determination of remaining characteristics is derived, treating void formation in the center region of a straight shaped line. In the region, current density and temperature can be regarded as being constant, and a handling of the parameter's formula is easy.

During the initial stage of electromigration damage, the atomic density gradient is assumed to be linear within the center region of the straight line. The product $\kappa \partial N / \partial x$ is determined as a characteristic constant depending on the line length.

The film characteristics $Q^*_{gb}[= Q^*_{gb}\_\sigma_T\Omega]$, Z^*, C^*_{gb} and $\kappa \partial N / \partial x$ are determined experimentally as follows. Accelerated tests are performed for a certain period of time. The line is subjected to input current density, j, under three different substrate temperatures, $Ts1$, $Ts2$ and $Ts3$. Then, let the temperature in the center region of the line be T_1, T_2 and T_3 in the cases when the substrate temperature is $Ts1$, $Ts2$ and $Ts3$, respectively. Let us denote each experimental condition as Condition_1: j_1 and T_1, Condition_2: j_1 and T_2, and Condition_3: j_1 and T_3. And also, the acceleration test is performed under a current density, j_4, which is different from j_1. Under this condition, the substrate temperature is controlled so that the temperature in the center region of the line, T_4, is approximately equal to T_2. Let us call this experimental condition Condition_4: j_4 and $T_4 (\cong T_2)$. In order to determine the substrate temperature, finite element method (FEM) analysis of the electrothermal problem is performed. The void volume is measured within the center region of the line after current stressing for a certain period of time.

On the other hand, considering the center region of the straight line, formula of AFD^*_{gen} is simplified by neglecting the terms associated with the gradients of temperature, current density and atomic density gradient in Eq. (2). The area of the center region, the line thickness, the net current_applying time and the atomic volume are multiplied by the simplified formula of AFD^*_{gen}. This product theoretically represents the volume of void to be formed. The net current_applying time is obtained by subtracting the incubation period from the current_applying time, where the incubation period is defined as the period from starting the electric current flow till the beginning of increase of electrical resistance due to void formation. The unknown film characteristics in AFD^*_{gen} can be obtained using the least_squares method. Namely, the characteristic constants are determined so that the following sum, F, takes a minimum value:

$$F = \sum_j \sum_i \left[\ln V_{ij} - \ln \left\{ A \times t_{ij} \times \text{thick} \times \frac{4}{\sqrt{3} d^2} \times \frac{C^*_{gb}}{T_j} exp\left(- \frac{Q^*_{gb}}{K T_j} \right) \left(Z^* e \rho_j j_j - \frac{\Omega}{N_0} \kappa \frac{\partial N}{\partial x} \right) \times \frac{\sqrt{3} \Delta \varphi}{\pi} \left\{ \sqrt{1 - \left(a_j \kappa \frac{\partial N}{\partial x} \right)^2} - a_j \kappa \frac{\partial N}{\partial x} \cos^{-1} \left(a_j \kappa \frac{\partial N}{\partial x} \right) \right\} \right\} \right]^2, \quad (3)$$

Where subscripts i and j represent the number of data measured in the experimental condition and the condition number respectively. Symbol V_{ij} is the measured void volume, A the area of the center region, t_{ij} the net current_applying time, thick the line_thickness, ρ_j the resistivity of the line at T_j and $a_j = \Omega d / (4 k T_j N_0 . .)$. The first and second terms in Eq. (3) represent void volume obtained experimentally and theoretical void volume, respectively.

4.2 Experiment

Two kinds of lengths of covered line were prepared. Al film was deposited by vacuum evaporation on the silicon with silicon oxide. The specimens were patterned by wet_etching and annealed at 673 K for 70 min. The density substrate cover surface was coated with polyimide and was annealed in N_2 to cure the polyimide layer. The dimensions of the specimen are shown in Fig. 1. The line whose length is 82 μm is called Sample L, and the line whose length is 32 μm is called Sample S.

Following the AFD^*_{gen}_based method to obtain the film characteristics, the acceleration tests were performed. At each of three kinds of substrate temperature, 458, 473 and 485 K, metal lines were subjected to the input D.C. current, the density of which was 5.5 MA/cm^2 (Condition_1, _2 and _3). In addition, the acceleration test (Condition_4) was performed under a current density of 8.5 MA/cm^2 in the case of Sample L, and 9.0 MA/cm^2 in the case of Sample S. In those cases, the substrate temperature was kept at 415 K so

that the temperature in the center region of the line was approximately equal to that of Condition_2. The twenty_five specimens were used in each testing condition. After direct current was applied, passivation film was removed by chemical etching, and the metal line was observed by field emission_scanning electron microscope (FE_SEM). The volume of the voids formed within the observed region was inferred by multiplying the film thickness to total area of the voids obtained by processing the FE_SEM image. By inputting the obtained void volumes to Eq. (3), the film characteristics were obtained as shown in Tab. 1.

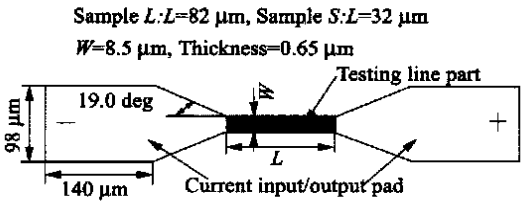

Fig. 1　Dimensions of metal line

Tab. 1　Film characteristics obtained by AFD^*_{gen}_based method

	Q^*_{gb}[eV]	Z^*	C^*_{gb}[$K\mu m^2/Js$]	$\kappa(\partial N/\partial x)$ [$J/\mu m^2$]
Sample *L*	0.505	− 8.7	1.15×10^{24}	− 0.366
Sample *S*	0.514	− 9.3	1.23×10^{24}	− 0.484

5　Numerical simulation of failure process

Lifetime and failure location in the passivated polycrystalline line are predicted by means of numerical simulation of the process, covering the building up of atomic density distribution, void initiation, void growth and line failure, using the governing parameter. The changes in current density and temperature distributions due to void growth are taken into account. In the simulation, the metal line to be predicted is divided into elements. The failure process is simulated by changing the thickness of each element based on the value of the governing parameter. The voids selectively grow along the grain boundary in polycrystalline lines, and they result in slit_like voids extending toward the line width and linking themselves. Considering this morphology of void growth, the element thickness is decreased only at very slim elements which are located based on measurements of the average grain size and the effective width of the slit_like void. We observed that the hillocks in the covered lines were collapsed by the passivation. Based on this fact, the increase of element thickness is conducted only at the elements neighboring on the slit_elements.

The calculation consists of the simulation part for an incubation period and that for a progress period of electromigration damage. In the simulation for the incubation period, at first, the distributions of current density and temperature in the line are obtained by two_dimensional FEM analysis. The parameter $AFD^*_{gb}\theta$ is calculated based on the results from this analysis and the film characteristic constants obtained in advance by the AFD^*_{gen}_based method. Since the angle θ in Eq. (2) takes an arbitrary value in practice, the parameter $AFD^*_{gb}\theta$ should be calculated considering the whole range of θ, *i. e.* from 0 to 2π. Then, the range of θ is divided by a sufficiently large number, n, and the values of $AFD^*_{gb}\theta$ are calculated at the respective range; $(2\pi/n)\cdot(m\_1) < \theta < (2\pi/n)\cdot m[m = 1, 2, \cdots, n]$. It can be supposed that each element has *n* pieces of segments and the respective range regarding θ is assigned to each segment. Let us call a piece of the segment 1/n_segment. The atomic density in each segment, N^*, is calculated based on the value of $AFD^*_{gb}\theta$, and the N^* values for all segments are averaged within each element to obtain the atomic density, N, of the element. The repetitive calculation for the simulation of the incubation period is carried out until the atomic density N^* in any 1/n_segment reaches a critical atomic density for void initiation, N^*_{min} or that for hillock initiation, N^*_{max}, and, in succession, the simulation of the damage_progress period is started with the atomic density distribution built up in the simulation of the incubation period.

In simulation of the progress period of the

damage, the values of N^* in all 1/n segments are calculated in the same manner as the simulation for the incubation period. Then, it is judged whether the atomic density N^* reaches N^*_{min} or N^*_{max}. when N^* is less than or equal to N^*_{min}($N^* \leqslant N^*_{min}$), the thickness of the slit_element is decreased based on deficiency of N^* under N^*_{min}. Conversely, when N^* is greater than or equal to N^*_{max}($N^* \geqslant N^*_{max}$), the thickness of the elements neighboring on the slit_element is increased according to the excess of N^* over N^*_{max}. On the other hand, when N^* is within N^*_{min} and N^*_{max}($N^*_{min} < N^* < N^*_{max}$), then N^* is regarded as not having reached the critical atomic density yet. Next, N^* of all 1/n_segments is averaged to obtain the atomic density N in each element, where the value of N^*_{min} is substituted for N^* if N^* is less than or equal to N^*_{min}, and the value of N^*_{max} is substituted for N^*, if N^* is greater than or equal to N^*_{max}. The atomic density gradient and its gradient are calculated based on the distribution of the atomic density N. The FEM analysis of current density and temperature in the line is carried out again considering each element thickness. The simulation for the period of the damage progress is carried out repeatedly until the line fails, which is defined as the state when the entire line width is occupied by elements whose temperature exceeds the melting point and/or elements penetrating the thickness. Here, the element thickness smaller than an infinitesimal threshold value is considered to be penetrating.

6 Verification of the prediction method

6.1 Prediction

Two passivated polycrystalline lines with different lengths shown in Fig. 1 were treated to predict the life time and failure location. For both samples, high current density (5.5 MA/cm^2) and high substrate temperature (473 K), relative to the general operating condition, were chosen as testing conditions to reduce the time required for the experiment of verification. The film characteristic constants for calculating the parameter $AFD^*_{gb}\theta$ have been obtained by the AFD^*_{gen}_based method as shown in Tab. 1.

By performing the numerical simulation using the obtained characteristics constants, the lifetime and the failure site were predicted for each sample. Prediction results are shown in Fig. 2 and Fig. 3. In the case of Sample L, the metal line failure was predicted to occur after 12 542 s lifetime, which is the sum of the incubation period(1 040 s) and the progress period of damage (11 502 s). The failure location was predicted to be near the cathodes end. On the other hand, in the case of Sample S, the failure was predicted to happen after 17 994 s lifetime. Which is the sum of the incubation period (1 440 s) and the progress period of damage (16 554 s). The failure location was predicted to be at the cathode end.

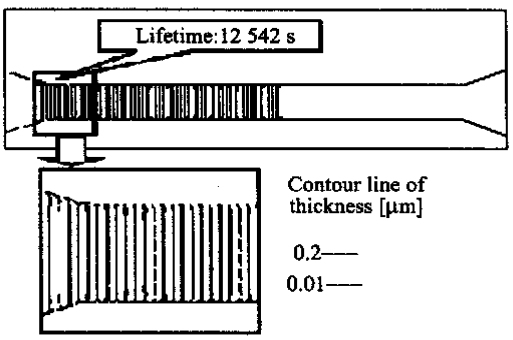

Fig. 2 Predicted results obtained with sample L

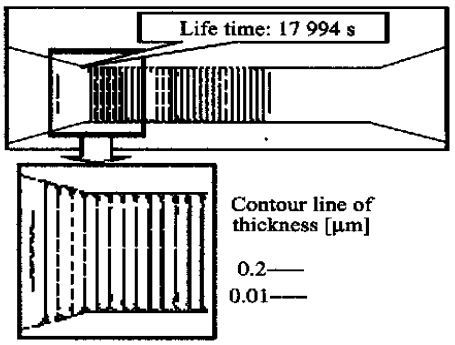

Fig. 3 Predicted result obtained with sample S

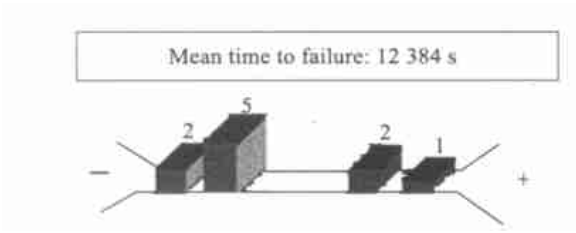

Fig. 4　Experimental results obtained with sample *L*

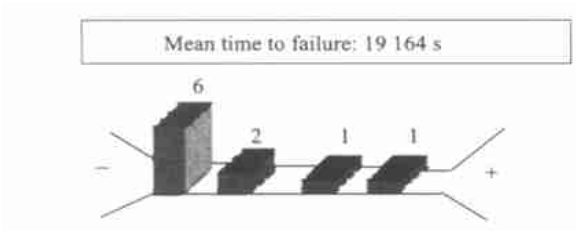

Fig. 5　Experimental results obtained with sample *S*

6.2　Experiment

In order to verify the results of the prediction, experiments were performed concerning the same line shape and under the same conditions as those in the prediction. The experiment was performed under the line specimen failed. The specimens were used for both Sample *L* and Sample *S*. After the lines became open, the passivation was removed by chemical etching and the specimens were observed by FE_SEM to detect the failure position.

Fig. 4 and Fig. 5 show the experimental results with frequency distribution of the failure site in the line and the mean time_to_failure. In the case of Sample *L*, the mean time_to_failure obtained from all the ten specimens was 12 384 s and the most frequent failure site was near the cathode side end of the line. On the other hand, the mean time_to_failure obtained from all the ten specimens was 19 164 s and the cathode side end was the most frequent site for Sample *S*.

Good agreement between the prediction and the experimental results was obtained concerning both lifetime and failure location. Though the failure site in the experiment was somewhat spread, the most frequent site was accurately predicted in both Sample *L* and Sample *S*. From this it was shown that once the film characteristics and operating condition were given, the lifetime and the failure location of a passivated polycrystalline line with any shape under arbitrary condition were able to be predicted.

7　Conclusions

A prediction method for electromigration failure in a passivated polycrystalline line was proposed using AFD^*_{gen}. In advance of the prediction, a method to determine film characteristics used in the prediction was shown based on AFD^*_{gen}. The AFD^*_{gen}_based method was applied to the passivated metal line with different line lengths and the film characteristics of these lines were obtained experimentally. Based on the obtained film characteristics, the lifetime and the failure site in the passivated polycrystalline lines were predicted by means of numerical simulation of the failure process. The predicted lifetimes agreed well with the experimental results for two metal lines with different line_lengths. Concerning the location of the failure, the most frequent site in the experiment agreed with the prediction result, though the experimentally obtained sites were somewhat spread. Thus, it has been shown that the present prediction method based on the governing parameter is able to predict accurately both the lifetime and the failure site of a passivated polycrystalline line.

REFERENCES:

[1] SASAGAWA K, NAKAMURA N, SAKA M, *et al*. Trans ASME J Elect Pack, 1998, 120: 360.
[2] SASAGAWA K, NAITO K, HASEGAWA M, *et al*. Advances in Electronic Packaging. 1999, ASME, EEP_26_1, 227 (1999).
[3] SASAGAWA K, NAITO K, SAKA M, *et al*. *J Appl Phys*, 1999, 86, 6043.
[4] SASAGAWA K, HASEGAWA M, NAITO K, *et al*. Thin Solid Films, 2001, 401: 255.
[5] SASAGAWA K, HASEGAWA M, SAKA M, *et al*. *J Appl Phys*, 2002, 91: 1882.